Polym. Bull. (2010) 65:669–680
DOI 10.1007/s00289-009-0241-x

ORIGINAL PAPER

Preparation and characterization of poly(ethylene glycol)/organo-vermiculite nanocomposite polymer electrolytes

Limin Zang · Jiahe Luo · Jinshan Guo · Hangong Liu · Jing Ru

Received: 1 September 2009 / Revised: 22 November 2009 / Accepted: 23 December 2009 /
Published online: 9 January 2010

Abstract Vermiculite (VMT) was readily intercalated by hexadecyl trimethyl ammonium bromide to yield organo-vermiculite (OVMT), which was confirmed by X-ray diffraction measurement and Fourier transform infrared spectroscopy. Poly(ethylene glycol)/organo-vermiculite (PEG/OVMT) nanocomposites were prepared by using the direct melt intercalation method, and its intercalation state was confirmed by transmission electron microscope. Thereafter, a lithium salt was dissolved in the PEG/OVMT nanocomposites to prepare composite polymer electrolytes. The highest conductivity was 2.1×10^{-5} S cm^{-1} at room temperature, which was obtained by AC impedance analysis when the amount of OVMT based on PEG was 1 wt%.

Keywords Polymer electrolytes · Vermiculite · Poly(ethylene glycol) · AC impedance

Introduction

Solid polymer electrolytes (SPE) are formed by dissolving salts in a polymer matrix. They have been receiving considerable attention as solid electrolyte materials for advanced applications, such as high energy density batteries, electrochromic

L. Zang · J. Luo · J. Guo (✉)
Institute of Polymer Science and Engineering, College of Chemistry and Chemical Engineering, Lanzhou University, Tianshui South Road 222#, Gansu 730000, China
e-mail: gjs@lzu.edu.cn

H. Liu · J. Ru
Gansu Research Institute of Chemical Industry, 730020 Lanzhou, China

H. Liu
Key Laboratory of Eco-Environment-Related Polymer Materials, Ministry of Education of China, 730000 Lanzhou, China

devices, chemical sensors, etc. Over the past 25 years, global interest has especially focused on lithium polymer electrolyte batteries because of their high energy density, safety, and the flexibility in both their shapes and production processes. A large number of studies to date have been carried out on poly(ethylene oxide) (PEO)-containing lithium salts [1–3].

In recent years, polymer/clay composites have attracted attention as new composite solid polymer electrolytes (CSPE) [4, 5]. It was reported that when the polymer was compounded with montmorillonite (MMT), the maximum value of the ionic conductivity based on CSPE reached 10^{-6} S cm^{-1} at 30 °C [4].

Vermiculite (VMT) like the well-known montmorillonite (MMT), as shown in Fig. 1, is a mica-type silicate and possesses a layered structure [6]. Because of the unique morphology and structure of VMT, it has been studied for the preparation of composites.

There have been some reports of the use of VMT in rubbers [7], building materials [8], plastic [9], silicateepoxy nanocomposite [10, 11]. It was found that the stacks of VMT sheets can be exfoliated and dispersed into individual layers, with a thickness of approximately 1 nm. The layers of VMT have the ability to have their surface chemistry fine-tuned through exchange reactions with organic and inorganic cations. Bridging flocculation and the interlayer structure of VMT with PEO mixtures have also been studied [12, 13]. However, there are no published data for the preparation of poly(ethylene glycol)/organo-vermiculite (PEG/OVMT) nanocomposite polymer electrolytes.

We select VMT as the host because of its important advantage: (a) VMT is a mica-type silicate and possesses a layered structure; (b) it is an inactive inorganic host without redox character, so the polymerization can be controlled; (c) it has a large surface area and strong absorptive capacity that is greater than any other natural minerals. The aim of this work was the preparation of PEG/OVMT nanocomposite polymer electrolytes by direct melt intercalation of PEG in OVMT.

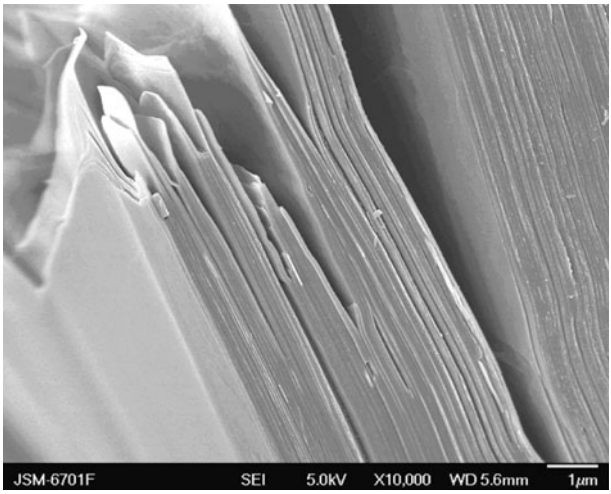

Fig. 1 SEM micrographs of raw vermiculite

The morphology and the mechanism of formation of the resulting PEG/OVMT nanocomposite polymer electrolytes were investigated.

Experimental

Materials

Vermiculite (VMT) with a cation exchange capacity (CEC) value of 120 mmol/100 g was purchased from Aldrich. It was heat treated for 12 h at 200 °C prior to use. Poly(ethylene glycol) (PEG) ($M_v = 20{,}000$ g/mol) was obtained from Sinopharm Chemical Reagent Co., Ltd and used after drying for 48 h in a vacuum oven at 70 °C. Lithium perchlorate ($LiClO_4$) was also obtained from Sinopharm Chemical Reagent Co., Ltd and used after drying for 48 h in a vacuum oven at 130 °C. Hexadecyl trimethyl ammonium bromide (HTAB) and lithium chloride (LiCl) were obtained from commercial suppliers and used directly without further purification.

Preparation of OVMT

Approximately, 10 g of the raw VMT was introduced into 600 ml of a 1 M HCl solution in a flask at room temperature. The resulting slurry was magnetically stirred for 8 h. Then VMT was separated by centrifuging and washing thoroughly with distilled water several times until the pH of the filtrate was 7.0. Following washing, VMT was dried at 160 °C overnight. The obtained fine VMT (1 g) was refluxed in about 200 ml of an aqueous solution containing LiCl (3 g) for 4 days at 50 °C, and the solution was changed four times everyday. At the end of the reaction, VMT was repeatedly washed with distilled water until no precipitate was obtained, after which $AgNO_3$ solution was added to the filtrate. Lithium-exchanged vermiculite (Li-VMT) (10 g) was then added to approximate 500 ml distilled water containing 32 g of HTAB and stirred for a week at 60 °C [14]. The resulting OVMT was repeated washed with distilled water until no precipitate was detected, after which $AgNO_3$ solution was added to the filtrate. The obtained OVMT was dried at 80 °C in a vacuum.

Preparation of nanocomposite solid polymer electrolytes (CSPE)

PEG was compounded with OVMT at 70 °C for 24 h to form the PEG/OVMT nanocomposites. The content of OVMT in PEG/OVMT nanocomposites was 0.5, 1, 2, and 5 wt%, respectively. Thereafter, the desired amount of $LiClO_4$ was added and dissolved in the PEG/OVMT nanocomposites at 70 °C for 4 h (molar ratio of O/Li was 16 [15]).

Characterization

The FTIR measurements (Impact 400, Nicolet, Waltham, MA) were carried out with the KBr pellet method. X-ray diffraction (XRD) patterns (Cu Kα-radiation) were

recorded with a Rigaku D-max/2400X diffractometer in range of $2\theta = 1 \sim 20°$ at room temperature, at a scanning speed and step size of 5°/min and 0.02°, respectively. Transmission electron microscope (TEM) were performed using a Hitachi H-600 at 100 kV, the specimens were solved in the ethanol and made by evaporating a drop of sample solutions on carbon-copper grids. AC impedance spectra was measured using LCR TH2818 automatic component analyzer, at scanning frequency range from 20 Hz to 300 kHz.

Results and discussion

Analysis of OVMT

Various methods have been proposed for the delamination of VMT. The classical methods are the acid-treatment method and the ion-exchange method [16, 17]. However, the acid-treatment method is poor for the preparation of PEG/VMT nanocomposites. It leads to poor compatibility between PEG and VMT, since PEG is organic matter and VMT is inorganic. Therefore, in this work, the ion-exchange method was adopted. We used 1 M HCl, and in acid-treatment time is 8 h, because too high a concentration or too long a treatment time may cause destruction of the crystal structure of VMT [16]. The acid-treated VMT was treated by using lithium-exchange method and HTAB-organized, respectively. In the spectrum of raw VMT shown in Fig. 2a, the peak at 997 cm^{-1} can be ascribed to asymmetric stretching vibrations of Si–O–Si and Si–O–Al; the bending vibration of Al–OH appeared at 819 cm^{-1}. The peaks at 1,635 and 3,420 cm^{-1} are assigned to hydration HOH and –OH vibrations. The spectrum of acid-treated VMT (Fig. 2b) and Li-VMT (Fig. 2c) are similar to the raw VMT. For the OVMT (Fig. 2d), C–H stretching vibration of alkyl chain appeared at 2,920 and 2,851 cm^{-1}, and C–H bending vibration appeared

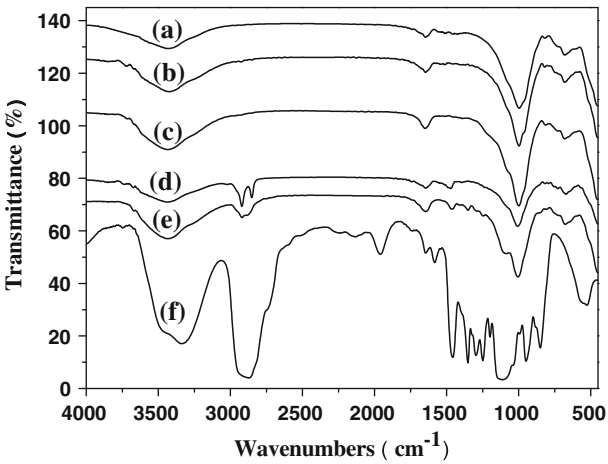

Fig. 2 FTIR spectrum of VMT (*a*) raw VMT, (*b*) acid-treated VMT, (*c*) Li-VMT, (*d*) OVMT, (*e*) PEG/OVMT nanocomposite, and (*f*) PEG

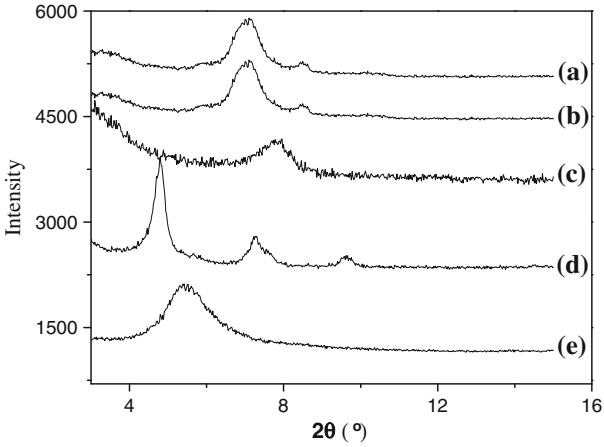

Fig. 3 XRD patterns of VMT (*a*) raw VMT, (*b*) acid-treated VMT, (*c*) Li-VMT, (*d*) OVMT, and (*e*) PEG/OVMT nanocomposite

at 1,472 cm^{-1}, which indicates OVMT was successfully synthesized. In Fig. 1f, the IR pesks of C–O–C stretching modes at 1,080–1,150 cm^{-1}, C–H stretching vibration 2,980 and 2,880 cm^{-1}, and C–H bending vibration appeared at 1,472 and 1,370 cm^{-1} for PEG existed, together with –OH stretching modes at 3,200–3,600 cm^{-1}. The same phenomenon appears in Fig. 1e. The new absorption band at 1,003 cm^{-1} (Fig. 1e) is attributed to Si–O–Si and Si–O–Al stretching vibrations. These results show the existence of OVMT in nanocomposites.

Figure 3 shows the XRD pattern of raw VMT, acid-treated VMT, Li-VMT, OVMT, and PEG/OVMT nanocomposite. As-received VMT (Fig. 3a) yielded characteristic diffraction peaks at $2\theta = 7.0°$ and 8.4° [16]. The acid-treated VMT (Fig. 3b) also has characteristic diffraction peaks at $2\theta = 7.0°$ and 8.4°, corresponding to the d-spacings of 1.25 and 1.04 nm, respectively. Li-VMT, however, has only one peak in the 2θ range from 0 to 15°, corresponding to a *d*-spacing of 1.13 nm (Fig. 3c), which is similar to Li-MMT [18]. The d-spacings decrease and become more uniform as other cations are replaced by Li^+. In Fig. 3c, OVMT yielded characteristic diffraction peaks at $2\theta = 4.8°$, 7.2°, and 9.5°, corresponding to the d-spacings of 1.84, 1.22, and 0.92 nm, respectively. The *d* value of 1.84 and 0.92 nm show that HTAB was partly intercalated into VMT ($d = 1.22$ nm belongs to the residual VMT). From the XRD pattern of nanocomposite (Fig. 3e), it suggests the formation of exfoliated structure, together with intercalated structure.

Analysis of PEG/OVMT nanocomposites

In general, the dispersion of layer particles in a polymer matrix can result in the formation of three types of phases, as illustrated in Fig. 4. Phase (a), exfoliated polymer–clay nanocomposite has low clay content and a monolithic structure. Intercalated clay composite (phase (b)) is formed by the insertion of a polymer into the layers of the host clay. As for conventional composites (phase (c)), the

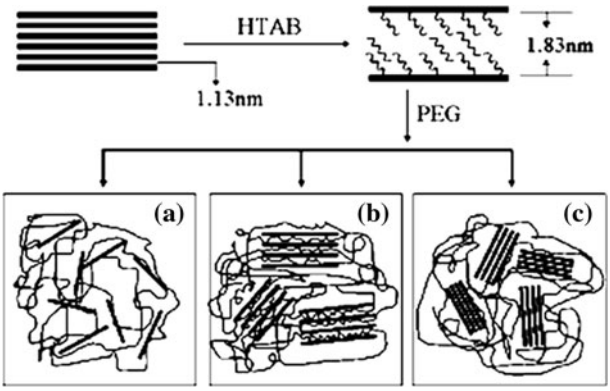

Fig. 4 Schematic illustration of the OVMT incorporation into the PEG matrix: (**a**) exfoliated, (**b**) intercalated, (**c**) conventional [19]

aggregated layers are simply dispersed as a segregated phase. Generally, there is more than one phase in a composite material. The dispersion of the clay particles in the polymer matrix depends on the clay content and properties of the polymer. In Fig. 5a and b, it can be seen that the stacks of OVMT were exfoliated within the PEG matrix and the OVMT sheets were dispersed within the PEG matrix irregularly. With the increase of OVMT content, however, a small amount of unexfoliated OVMT layers exist as clusters shown in Fig. 5c and d. In this sense, the PEG/OVMT nanocomposite can be considered to be a mixed exfoliated/intercalated system (Fig. 4a, b). Presumably, the edges of OVMT are more accessible intercalation for the PEG chains than the center. Because of the shape of the OVMT layers, PEG molecular chains must enter the galleries from the agglomerate polymer melt to the primary OVMT particles, and further to the edges of OVMT layers. OVMT crystallites on the interior side of the front remained unintercalated. Therefore, it leads to take on phase (b) and phase (c).

Conductivity of PEG/OVMT CSPE

The ionic conductivity of the CSPE was analyzed by their AC impedance spectra. The dependence of the AC impedance plots SS|SPE|SS sandwiched structures are shown in Fig. 6. Except for Fig. 6c, each spectrum shows a compressed semicircle in the high frequency range and an inclined straight line in the low frequency range, which is different from the Li non-blocking electrode. For the Li non-blocking electrode [20], there are two semicircles at high and inter-mediate frequencies and a spur in the low frequency range. In our experiment, only one semicircle was observed, which indicates that there was no electrode reaction at the electrode/electrolytes interfaces. The high frequency semicircle, as reported, represents the bulk relaxation of the SPE films as CSPE, while the straight line after the semicircle is due to the migration of ions and the surface in-homogeneity

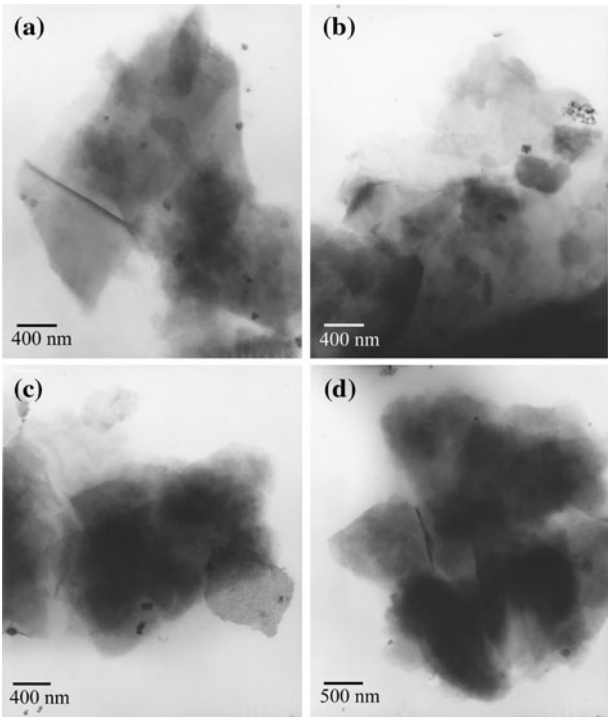

Fig. 5 TEM micrographs of CSPE: **a** 0.5 wt% OVMT, **b** 1 wt% OVMT, **c** 2 wt% OVMT, and **d** 5 wt% OVMT

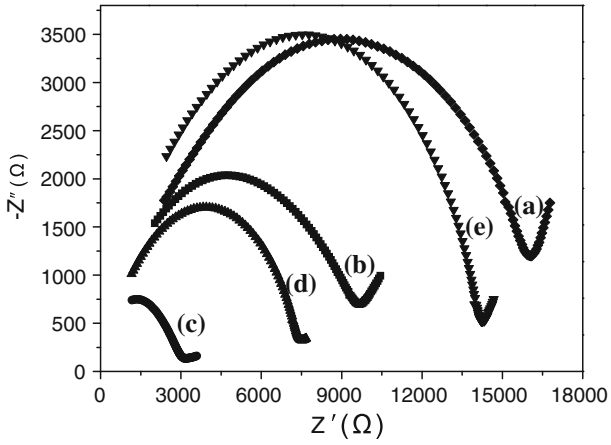

Fig. 6 AC impedance spectra of CSPE: (*a*) pure PEG, (*b*) 0.5 wt% OVMT, (*c*) 1 wt% OVMT, (*d*) 2 wt% OVMT, and (*e*) 5 wt% OVMT

of the electrodes [21]. In Fig. 6c, it can be seen that the high frequency semicircle was reduced. The main reason is that the ionic conductivity is due to the migration of ions offering [22, 23].

The ionic conductivity (δ) was calculated from the bulk resistance (R_b) found in the AC impedance spectra. In Fig. 6, the low frequency end of the semicircle and the high frequency end of the straight line coincide with the bulk resistance of the CSPE. The ionic conductivity of the samples can be then calculated by the following equation:

$$\delta = d/(R_b \cdot S)$$

where d is the thickness of the CSPE thin film, R_b is the bulk resistance, S is the area of SS electrodes contacting with the CSPE film. Table 1 shows the relative values for calculating the ionic conductivity. It is found that the conductivity of PEG/OVMT CSPE first increased and then decreased with the addition of OVMT at room temperature. The highest conductivity among the PEG/OVMT CSPE samples is 2.1×10^{-5} S cm^{-1} when the amount of OVMT based on PEG was 1 wt%.

It has been reported that the extent to which the platelets are intercalated or exfoliated is expected to play a distinct role in the conductivity of these nanocomposites. A completely exfoliated morphology is expected to yield the highest conductivity since more Li cations would be mobile and available for conduction. Conversely, a system in which the Li cations are trapped between intercalated platelets would not be nearly as conductive [24]. In this work, OVMT was best exfoliated in PEG matrix when the amount of OVMT was low, as shown in Fig. 4. Each silicate layer possesses numerous negative charges, and interacts with lithium cations as a Lewis acid–base [25]. Therefore, the interaction of lithium cations and PEG was weakened, which leads to enhancement of the number of charge carriers [26]. The overall reactions will lead to the increase of the ionic conductivity. Figure 7 shows the schematic illustrations of the interactions of PEG and OVMT with lithium salt. However, it was found to increase the silicate aggregation tendency with increasing OVMT concentration. The mobility of lithium ions was restricted by the additional negative charges provided by more silicate layers. Thus, it leads to the decrease in ionic conductivity of CSPE [4].

In the log δ versus $1/T$ plot, as shown in Fig. 8, the ionic conductivity increases with increasing temperature in the nanocomposite polymer electrolytes based on 1 wt% OVMT. The tendency is essentially linear, meaning that the temperature dependence of the ionic conductivity follows the "Vogel–Tammann–Fulcher" (VTF) equation, namely,

Table 1 Relative values of CSPE for calculating the ionic conductivity

OVMT (wt%)	0	0.5	1	2	5
d (μm)	225	245	180	245	225
S (cm^2)	0.2826	0.2826	0.2826	0.2826	0.2826
R_b (Ω)	16,070	9,690	3,098	7,530	14,260
δ (S cm^{-1})	5.0×10^{-6}	8.9×10^{-6}	2.1×10^{-5}	1.2×10^{-5}	5.6×10^{-6}

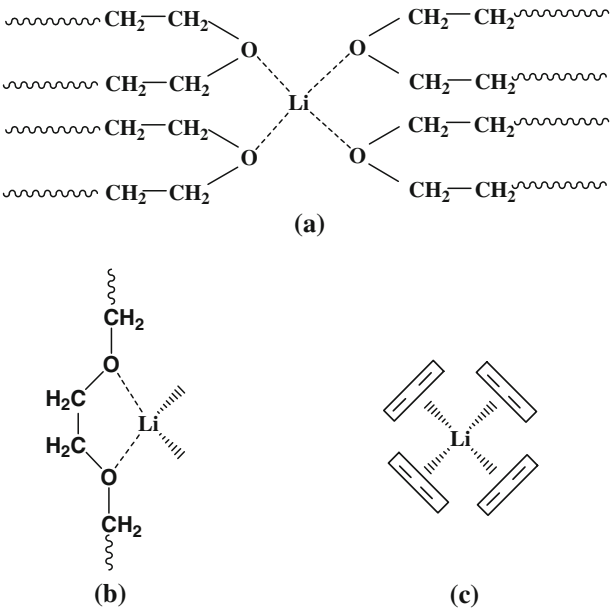

Fig. 7 Schematic illustrations of the complex formed by Li^+ with **a** PEG, **b** PEG and silicate layers, and **c** silicate

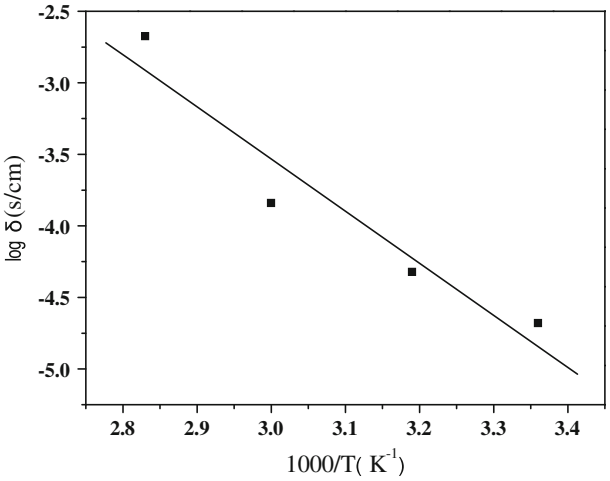

Fig. 8 VTF plot for CSPE based on 1 wt% OVMT

$$\delta = AT^{-1/2}\exp\left[-E_b/\left(T - T_g\right)\right]$$

in which A and E_b are fitting constants and T_g is related to the equilibrium state glass transition temperature, indicating that the ion transport was correlated with the segmental motion of the polymer chain [27]. In Fig. 9, the bulk resistance of the

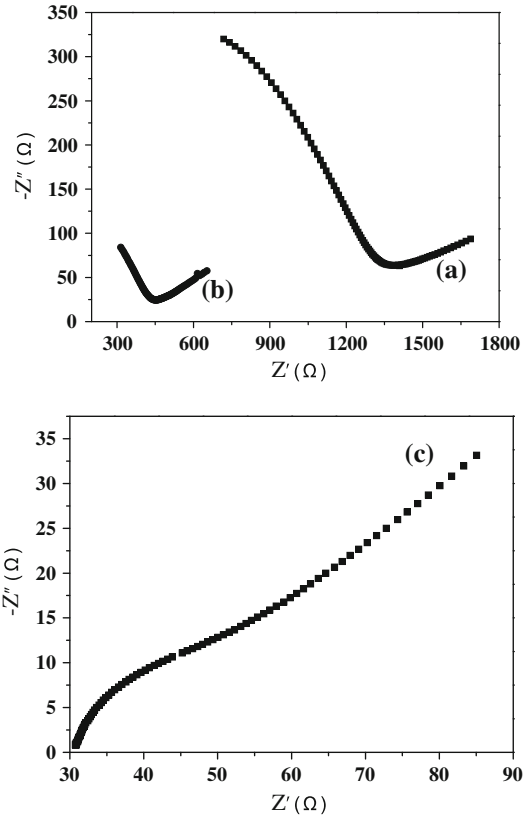

Fig. 9 AC impedance spectra of CSPE based on 1 wt% OVMT in (*a*) 40 °C, (*b*) 60 °C, and (*c*) 80 °C

polymer electrolytes decreases with increasing temperature, and the high frequency semicircle gradually reduce. In simple, the energy of ions transfer was reduced due to the increased segmental motion of the polymer chain, which is reflected in the ionic conductivity.

Conclusions

This work represents the preparation of PEG/OVMT nanocomposite polymer electrolytes. VMT can be readily intercalated by HTAB to yield OVMT. PEG was then direct melt intercalated into the OVMT. The obtained PEG/OVMT nanocomposites can result in the formation of three types of phases (exfoliated, intercalated and conventional). The room temperature ionic conductivity of PEG/OVMT nanocomposite polymer electrolytes can be enhanced with the addition of OVMT. The highest conductivity was 2.1×10^{-5} S cm^{-1} when the amount of OVMT based on PEG was 1 wt%, enhanced nearly four times compared with pure PEG electrolytes. The ionic conductivity versus temperature plot follows the VTF equation. We suggest that polymer/vermiculite nanocomposite polymer electrolytes will have great potential in the research field of CSPE.

References

1. Li Q, Sun HY, Takeda Y, Imanishi N, Yang J, Yamamoto O (2001) Interface properties between a lithium metal electrode and a poly(ethylene oxide) based composite polymer electrolyte. J Power Sources 94(2):201–205
2. Hyun JK, Dong H, Christopher RP, Frech R, Wheeler RA (2001) Molecular dynamics simulations and spectroscopic studies of amorphous tetraglyme ($CH_3O(CH_2CH_2O)_4CH_3$) and tetraglyme: $LiCF_3SO_3$ structures. J Phys Chem B 105(16):3329–3337
3. Lee YG, Ryu KS (2004) Preparation and characterization of asymmetric composite polymer electrolytes for lithium metal polymer batteries. Polym Bull 51(4):315–320
4. Wang XJ, Kang JJ, Wu YP, Fang SB (2003) Novel composite polymer electrolytes based on poly(ether-urethane) network polymer and modified montmorillonite. Electrochem Commun 5(12):1025–1029
5. Sandí G, Carrado KA, Joachin H, Lu WQ, Prakash J (2003) Polymer nanocomposites for lithium battery applications. J Power Sources 119–121:492–496
6. Ibrahim MA, Lee BG, Park NG (1999) Synthesis of new oligothiophene derivatives and their intercalation compounds: orientation effects. Synth Met 105(1):35–42
7. Zhang Y, Liu W, Han W, Guo W, Wu C (2009) Preparation and properties of novel natural rubber/organo-vermiculite nanocomposites. Polym Compos 30(1):38–42
8. Akao M, Yamazaki A, Fukuda Y (2003) Vermiculite board for novel building material. J Mater Sci Lett 22(21):1483–1485
9. Zhang JH, Zhuang W, Zhang Q, Liu B, Wang W, Hu BX, Shen J (2007) Novel polylactide/vermiculite nanocomposites by in situ intercalate polymerization. I. Preparation, characterization, and properties. Polym Compos 28(4):545–550
10. Tjong SC, Meng YZ, Xu Y (2002) Structure and properties of polyamide-6/vermiculite nanocomposites prepared by direct melt compounding. J Polym Sci B 40(24):2860–2870
11. Campos AM, Moreno S, Molina R (2008) Relationship between hydrothermal treatment parameters as a strategy to reduce layer charge in vermiculite, and its catalytic behavior. Catal Today 133(1–4):351–356
12. Smalley MV, Hatharasinghe HLM, Osborne I, Swenson J, King SM (2001) Bridging flocculation in vermiculite–PEO mixtures. Langmuir 17(13):3800–3812
13. Swenson J, Smalley MV, Hatharasinghe HLM, Fragneto G (2001) Interlayer structure of a clay-polymer-salt-water system. Langmuir 17(13):3813–3818
14. Xu J, Li RKY, Xu Y, Li L, Meng YZ (2005) Preparation of poly(propylene carbonate)/organo-vermiculite nanocomposites via direct melt intercalation. Eur Polym J 41(4):881–888
15. Angell CA, Liu C, Sanchez E (1993) Rubbery solid electrolytes with dominant cationic transport and high ambient conductivity. Nature 362(6416):137–139
16. Xu J, Meng YZ, Li RKY, Xu Y, Rajulu AV (2003) Preparation and properties of poly(vinylalcohol)–vermiculite nanocomposites. J Polym Sci B 41(7):749–755
17. Burnside SD, Wang HC, Giannelis EP (1999) Direct polymer intercalation in single crystal vermiculite. Chem Mater 11(4):1055–1060
18. Kim S, Park SJ (2007) Preparation and ion-conducting behaviors of poly(ethylene oxide)-composite electrolytes containing lithium montmorillonite. Solid State Ion 178(13–14):973–979
19. Lan T, Kaviratna PD, Pinnavaia TJ (1995) Mechanism of clay tactoid exfoliation in epoxy-clay nanocomposites. Chem Mater 7(11):2144–2150
20. Groce F, Gerace F, Dautzemberg G, Passerini S, Appetecchi GB, Scrosati B (1994) Synthesis and characterization of highly conducting gel electrolytes. Electrochim Acta 39(14):2187–2194
21. Pickup PG (1990) Alternating current impedance study of a polypyrrole-based anion-exchange polymer. J Chem Soc Faraday Trans 86:3631–3636
22. Jacob MME, Prabaharan SRS, Radhakrishna S (1997) Effect of PEO addition on the electrolytic and thermal properties of PVDF-$LiClO_4$ polymer electrolytes. Solid State Ion 104(3–4):267–276
23. Sørensen PQ, Jacobsen T (1983) Phase diagram and conductivity of the polymer electrolyte: $PEORLiCF_3SO_3$. Polym Bull 9:47–51
24. Walls HJ, Riley MW, Singhal RR, Spontak RJ, Fedkiw PS, Khan SA (2003) Nanocomposite electrolytes with fumed silica and hectorite clay networks: passive versus active fillers. Adv Funct Mater 13(9):710–717

25. Chen HW, Chang FC (2001) The novel polymer electrolyte nanocomposite composed of poly(ethylene oxide), lithium triflate and mineral clay. Polymer 42(24):9763–9769
26. Lee BH, Choi NS, Park JK (2002) Effect of silica on the interfacial stability of the PEO based polymer electrolytes. Polym Bull 49:63–68
27. Okamoto Y, Yeh TF, Lee HS, Skotheim TA (1993) Design of alkaline metal ion conducting polymer electrolytes. J Polym Sci A 31(10):2573–2581